

## Appendix 4.A Minimal requirements for a consistent mean field theory

In what follows the question of why, rigorously speaking, one cannot talk about single-particle motion, let alone spectroscopic factors, not even within the framework of Hartree-Fock theory, is briefly touched upon (see also App. 4.I).

As can be seen from Fig. 4.A.1 the minimum requirements of selfconsistency to be imposed upon single-particle motion requires both non-locality in space (HF) and in time (TDHF)

$$i\hbar \frac{\partial \varphi_v}{\partial t} = -\frac{\hbar^2}{2m} \nabla^2 \varphi_v(x, t) + \int dx' dt' U(x - x', t - t') \varphi_v(x', t'), \quad (4.A.1)$$

and consequently also of collective vibrations and, consequently, from their interweaving to dressed single-particles (quasiparticles), let alone renormalized collective modes (cf. Fig. 4.C.3). Assuming for simplicity infinite nuclear matter (confined by a constant potential of depth  $V_0$ ), and thus plane wave solutions, the above time-dependent Schrödinger equation leads to the quasiparticle dispersion relation

$$\hbar\omega = \frac{\hbar^2 k^2}{2m^*} + \frac{m}{m^*} V_0, \quad (4.A.2)$$

where the effective mass

$$m^* = \frac{m_k m_\omega}{m}, \quad (4.A.3)$$

in the product of the  $k$ -mass

$$m_k = m \left( 1 + \frac{m}{\hbar^2 k} \frac{\partial U}{\partial k} \right)^{-1}, \quad (4.A.4)$$

closely connected with the Pauli principle ( $\frac{\partial U}{\partial k} \approx \frac{\partial U_x}{\partial k}$ ), while the  $\omega$ -mass

$$m_\omega = m \left( 1 - \frac{\partial U}{\partial \hbar\omega} \right), \quad (4.A.5)$$

results from the dressing of the nucleon through the coupling with the (quasi) bosons. Because typically  $m_k \approx 0.7m$  and  $m_\omega \approx 1.4m$   $m^* \approx m$ , one could be tempted to conclude that the results embodied in the dispersion relation (4.A.2) reflects the fact that the distribution of levels around the Fermi energy can be described in terms of the solutions of a Schrödinger equation in which nucleons of mass equal to the bare nucleon mass  $m$  move in a Saxon-Woods potential of depth  $V_0$ .

Now, it can be shown that the occupancy of levels around  $\varepsilon_F$  is related to  $Z_\omega$ , a quantity which measures the discontinuity at the Fermi energy (Fig. 4.A.1 (h)) and which is equal to  $m/m_\omega = 1/(1+\lambda_{p-v}) \approx 0.7$ ,  $\lambda_{p-v}$  being the mass enhancement factor ( $\lambda_{p-v} = N(0)g_{p-v}$ ), product of the density of levels at the Fermi energy and

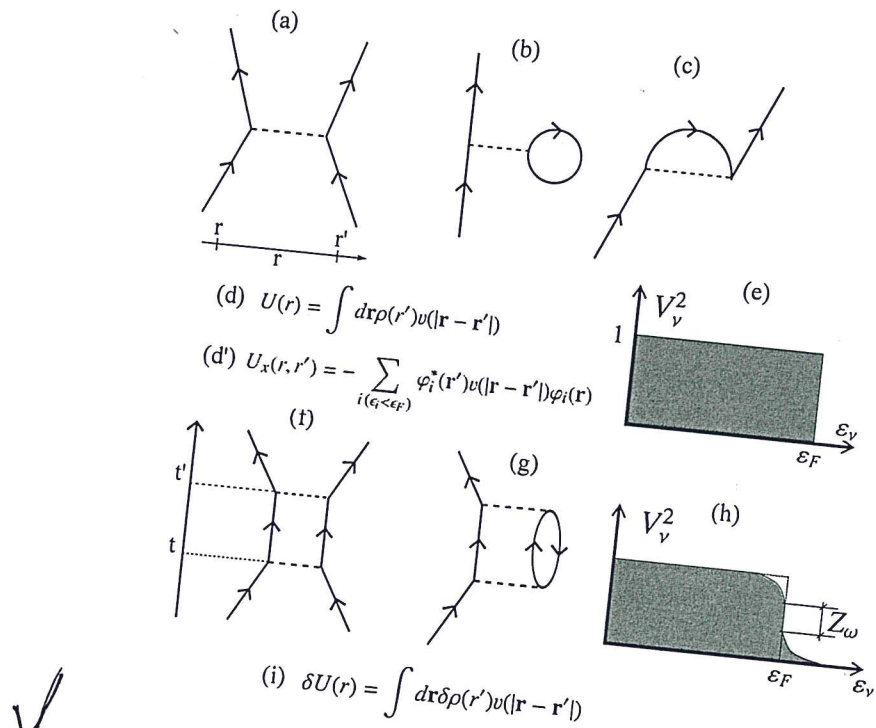
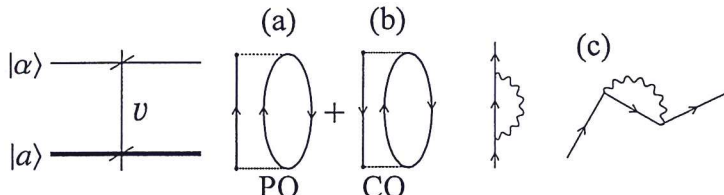


Figure 4.A.1: (a) Scattering of two nucleons through the bare  $NN$  interaction  $v(|\mathbf{r} - \mathbf{r}'|)$ , (b) contribution to the direct ( $U$ , Hartree) and (c) to the exchange ( $U_x$ , Fock) potential, resulting in (d) the (static) self-consistent relation between potential and density (non-local (d')), which (e) uncouples occupied ( $\epsilon_\nu \leq \epsilon_F$ ) from empty states ( $\epsilon_\nu > \epsilon_F$ ), (f) multiple scattering of two nucleons lead, through processes like the one depicted in (g), eventually propagated to all orders, to: (h) softening of the discontinuity of the occupancy of levels at  $\epsilon_F$ , as well as to: (i) generalization of the static selfconsistency into a dynamic relation encompassing also collective vibrations (Time-Dependent HF solutions of the nuclear Hamiltonian, conserving energy weighted sum rules (EWSR)).

do not break  $v(\vec{r} - \vec{r}', | \cdot |)$



✓ Figure 4.B.1: Two state schematic model describing the breaking of the strength of the pure single-particle state  $|a\rangle$ , through the coupling to collective vibrations (wavy line) associated with polarization (PO) and correlation (CO) processes.

*directly*

the particle-vibration coupling parameter (cf. e.g. Bohr, A. and Mottelson (1975); Brink, D. and Broglia (2005) and refs. therein). This is in keeping with the fact that the time the nucleon is coupled to the vibrations it cannot behave as a single-particle and can thus not contribute to e.g. the single-particle pickup cross section.

It is of notice that the selfconsistence requirements for the iterative solution of Eq. (4.A.1) (see Fig. 4.A.1 (d) and (d')) remind very much those associated with the solution of the Kohn-Sham equations in finite systems,

$$H^{KS} \varphi_\gamma(\mathbf{r}) = \lambda_\gamma \varphi_\gamma(\mathbf{r}), \quad (4.A.6)$$

where

$$H^{KS} = -\frac{\hbar^2}{2m_e} \nabla^2 + U_H(\mathbf{r}) + V_{ext}(\mathbf{r}) + U_{xc}(\mathbf{r}), \quad (4.A.7)$$

$H^{KS}$  being known as the Kohn-Sham Hamiltonian,  $V_{ext}(\mathbf{r})$  being the field created by the ions and acting on the electrons. Both the Hartree and the exchange-correlation potentials  $U_H(\mathbf{r})$  and  $U_{xc}(\mathbf{r})$  depend on the (local) density, hence on the whole set of wavefunctions  $\varphi_\gamma(\mathbf{r})$ . Thus, the set of  $KS$ -equations must be solved selfconsistently (Broglia et al., 2004) and refs. therein).

## Appendix 4.B Model for single-particle strength function: Dyson equation

In the previous Appendix we schematically introduced arguments regarding the “impossibility” of defining a “bona fide” single-particle spectroscopic factor. It was done with the help of Feynman (NFT) diagrams. In what follows we essentially repeat the arguments, but this time in terms of Dyson’s (Schwinger) language. For simplicity, we consider a two-level model where the pure single-particle state  $|a\rangle$  couples to a more complicated (doorway) state  $|\alpha\rangle$ , made out of a fermion (particle or hole), coupled to a particle-hole excitation which, if iterated to all orders can give rise to a collective state (Fig. 4.B.1). The Hamiltonian describing the system is (Bohr and Mottelson, 1969)

$$H = H_0 + v, \quad (4.B.1)$$

\*)

\*\*) See e.g.

\*\*\*)

where

$$H_0|a\rangle = E_a|a\rangle, \quad (4.B.2)$$

and

$$H_0|\alpha\rangle = E_\alpha|\alpha\rangle. \quad (4.B.3)$$

Let us call  $\langle a|v|\alpha\rangle = v_{a\alpha}$  and assume  $\langle a|v|a\rangle = \langle \alpha|v|\alpha\rangle = 0$ .

From the secular equation

$$\begin{pmatrix} E_\alpha & v_{a\alpha} \\ v_{a\alpha} & E_a - E_i \end{pmatrix} \begin{pmatrix} C_\alpha(i) \\ C_a(i) \end{pmatrix} = 0, \quad (4.B.4)$$

and associated normalization condition

$$C_a^2(i) + C_\alpha^2(i) = 0, \quad (4.B.5)$$

one obtains

$$C_a^2(i) = \left( 1 + \frac{v_{a\alpha}^2}{(E_\alpha - E_i)^2} \right)^{-1}, \quad (4.B.6)$$

and

$$\Delta E_a(E) = E_a - E = \frac{v_{a\alpha}^2}{E_\alpha - E}. \quad (4.B.7)$$

The energy of the correlated state

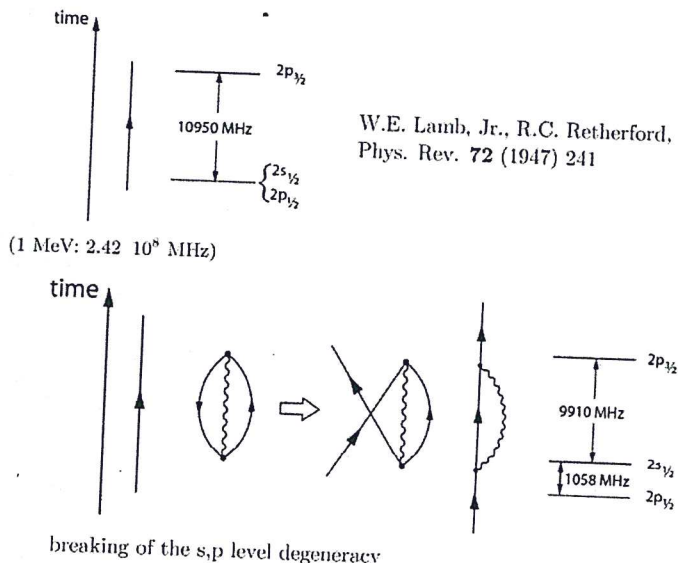
$$|\tilde{a}\rangle = C_a(i)|a\rangle + C_\alpha(i)|\alpha\rangle, \quad (4.B.8)$$

is obtained by the (iterative) solution of the Dyson equation (4.B.7), which propagate the bubble diagrams shown in Figs 4.B.1 (a) and (b) to infinite order leading to collective vibrations (see Fig. 4.B.1 (c))

With the help of the definition given in eq (4.A.5), and making use of the fact that in the present case, the quantity  $U$  appearing in this equation coincides, within the present context with  $\Delta E_a(E)$ , one obtains that the discontinuity of the single-particle levels at the Fermi energy is given by

$$Z_\omega = C_a^2(i) = \left( \frac{m_\omega}{m} \right)^{-1}. \quad (4.B.9)$$

Making use of the solution of the Dyson equation (4.B.7), and of the relations (4.B.5) and (4.B.6), one can calculate the renormalized state  $|\tilde{a}\rangle$  (Eq. 4.B.8) to be employed in working out the associated, modified, single-particle transfer form factor needed in the calculation of the absolute value of one-particle transfer cross sections (cf. e.g. Sect. 4.2.1, where the above concepts and techniques are applied to the study of one-neutron transfer reactions in open shell, superfluid ( $^{120}\text{Sn}$ )).



✓ Figure 4.D.1: Schematic representation of the processes associated with the Lamb shift.

ically, few MeV (low-lying collective vibrations of which one has to add dipole pigmy resonances ( $\hbar\omega_{\text{pigmy}} \leq 1$  MeV) as for example that involved in the glue of the halo neutrons of  $^{11}\text{Li}(\text{gs})$  (cf. App. D), and tens of MeV (giant resonances), leading to a rich number of CO and PO processes. This is in keeping with the fact that the intermediate boson (photon QED, vibrations of nuclear medium) propagates in a medium which is not isotropic, thus undergoing fragmentation of the associated strength (inhomogeneous damping). To make even richer the nuclear scenario, collisional damping plays also a role in the strength function of GR. Nonetheless, the associated widths (lifetimes) are controlled by the coupling to doorway states (cf. figures 1.6 and 4.E; cf. also App. 4.D, introducción), even at nuclear temperatures of 1–2 MeV, let alone when the GR is based on the ground state (Fig. 4.C.3; cf. Bortignon, P.F. et al. (1998) and refs. therein, cf. also Broglia, R.A. et al. (1987)). The strong cancellation found between self-energy and vertex correction diagrams, testify to the collectivity of nuclear vibrations (generalized Ward identities), and reminds of Furry's theorem (no coupling between one- and two-photon states). Summing up, nothing is really free in the quantal world (cf. App. 4.E). Selected measurements carried out with specific probes, can make virtual processes become real, and shed light on the variety of these processes leading to renormalized elementary modes of nuclear excitation (dressed fermions and bosons).

*mechanisms*

\*.)

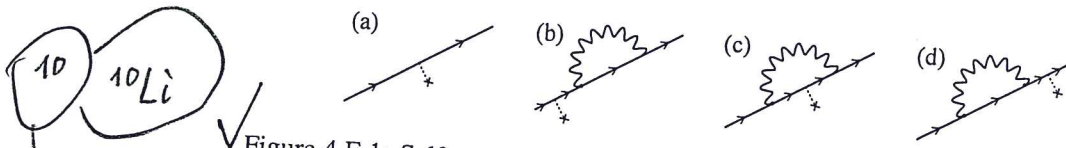


Figure 4.E.1: Self energy (effective-mass-like) processes. The result of the probing with an external field (dotted line started with a cross, observer) of the properties (mass, single-particle energy, etc) of a fermion (e.g. an electron or a nucleon, arrowed line) dressed through the coupling of (quasi) bosons (photons or collective vibrations, wavy line), corresponds to the modulus squared of the sum of the amplitudes associated with each of the four diagrams (a)–(d) (cf. (Feynman, 1975)). A concrete embodiment of the above parlance is provided by the process  ${}^1\text{H}({}^{11}\text{Li}, {}^0\text{Li})^2\text{H}$  (cf. Figs. 4.2.5 and 4.2.6).

## Appendix 4.D The Lamb Shift

In Fig. 4.D.1 we display a schematic summary of the electron–photon processes, associated with Pauli principle corrections, leading to the splitting of the lowest  $s, p$  states of the hydrogen atom known as the Lamb shift.

In the upper part of the figure the predicted position of the electronic single-particle levels of the hydrogen atom as resulting from the solution of the Schrödinger equation (Coulomb field). In the lowest part of the figure one displays the electron of an hydrogen atom (upwards going arrowed line) in presence of vacuum ZPF (electron–positron pair plus photon, oyster-like diagram) (within this scenario we refer to App. 4.C concerning to the central role ZPF of the vacuum and the concept of antiparticle (hole) has in the description of physical, dressed-observable states of quantal many-body systems). Because the associate electron virtually occupies states already occupied by the hydrogen's electron, thus violating Pauli principle, one has to antisymmetrize the corresponding two-electron state. Such process gives rise to the exchange of the corresponding fermionic lines and thus to CO-like diagrams as well as, through time ordering, to PO-like diagrams. The results provide a quantitative account of the experimental findings.

## Appendix 4.E Self-energy and vertex corrections

In Fig. 4.E.1 an example of the fact that in field theories (e.g. QED or NFT), nothing is really free and that e.g., the bare mass of a fermion (electron or nucleon), is the parameter one adjusts ( $m_k$ ) so that the result of a measurement gives the observed mass (single particle energy). In Fig. 4.E.2, lowest order diagrams associated with the renormalization of the fermion–boson interaction (vertex corrections) are given. The sum of contributions (a) and (b) can, in principle, be represented by a renormalized vertex (cf. diagram (c)). It is of notice, however, that there is, as a rule, conspicuous interference (e.g. cancellation) in the nuclear case between

~~Lamb and Rutherford  
Kroll and Lamm~~

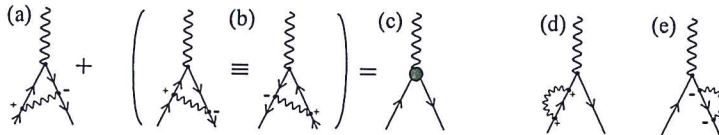


Figure 4.E.2: Vertex corrections. These are triple-interaction diagrams (phonon, particle and hole lines) in which none of the incoming lines can be detached from either of the other two by cutting one line. In connection with condensed matter Migdal's theorem (Migdal (1958)) states that for phonons, (Bardeen and Pines (1955), Fröhlich, H. (1952)) vertex corrections can be neglected (cf. also Anderson (1984)). Vertex corrections are, as a rule, important in the nuclear case where they lead to conspicuous cancellations of the self-energy contributions (cf. e.g. Bortignon et al. (1983), cf. also Anderson (1984)). The solid grey circle in (c) represents the effective, renormalized vertex.

*see*  
 vertex and self-energy contributions (diagrams (a) and (d)+(e) of Fig. 4.E.2, a phenomenon closely related with conservation laws (generalized Ward identities) cf. e.g. Schrieffer (1964)); cf. also Fig. 4.C.3 and refs. Bortignon and Broglia (1981); Bertsch et al. (1983) and Bortignon, P.F. et al. (1998) pp. 82–86). In particular, cancellation in the case in which the bosonic modes are isoscalar (Bortignon et al., 1983). Consequently, one has to sum explicitly the different amplitudes with the corresponding phases and eventually take the modulus squared of the result to eventually obtain the quantities to be compared with the data, a fact that precludes the use of an effective,  $\omega$ -independent (renormalized) vertex.

Within the framework of QED the above mentioned cancellations are exact implying that the interaction between one- and two-photon states vanishes (Furry theorem). The physics at the basis of the cancellation found in the nuclear case can be exemplified by looking at a spherical nucleus displaying a low-lying collective quadrupole vibration. The associated zero point fluctuations (ZPF) lead to time dependent shapes with varied instantaneous values of the quadrupole moment, and of its orientation (dynamical spontaneous breaking of rotational invariance) (ver. appendix 1B correlations and fluctuations). In other words, a component of the ground state wavefunction ( $(|j_p \otimes j_h^{-1} 2^+ \otimes 2^+; 0^+\rangle)$ , which can be viewed as a gas of quadrupole (quasi) bosons promoting a nucleon across the Fermi energy (particle-hole excitation) will lead to fermionic states which behave as having a positive (particle) and a negative (hole) effective quadrupole moment, in keeping with the fact that the closed shell system is spherical, thus carrying zero quadrupole moment.

\* )  
 \*\* ) ←

above

### Appendix 4.F Single-nucleon transfer for pedestrians

In this Appendix we discuss some aspects of the relations existing between nuclear structure and one-particle transfer cross sections. To do so, we repeat some of the steps carried out in the text but this time in a simpler and straightforward way, ignoring the complications associated with the spin carried out by the particles, the spin-orbit dependence of the optical model potential, the recoil effect, etc.

We consider the case of  $A(d, p)A+1$  reaction, namely that of neutron stripping. The intrinsic wave functions  $\psi_\alpha$  and  $\psi_\beta$ , where  $\alpha = (A, d)$  and  $\beta = ((A+1), p)$ ,

$$\psi_\alpha = \psi_{M_A}^{I_A}(\xi_A) \phi_d(\vec{r}_{np}), \quad (4.F.1a)$$

$$\begin{aligned} \psi_\beta &= \psi_{M_{A+1}}^{I_{A+1}}(\xi_{A+1}) \\ &= \sum_{l, I'_A} (I'_A; l) I_{A+1} [\psi_{M_A}^{I_A}(\xi_A) \phi_l(\vec{r}_n)]_{M_{A+1}-M_A}^{I_{A+1}}, \end{aligned} \quad (4.F.1b)$$

where  $(I'_A; l) I_{A+1}$  is a generalized fractional parentage coefficient. It is of notice that this fractional parentage expansion is not well defined. In fact, as a rule,  $(I'_A; l) I_{A+1} \phi_l(\vec{r}_n)_{M_{A+1}-M_A}$  is an involved, dressed quasiparticle state containing only a fraction of the "pure" single particle strength (cf. Apps 4.A and 4.B). For simplicity we assume the expansion to be operative. To further simplify the derivation we assume we are dealing with spinless particles. This is the reason why no "intrinsic" proton wavefunction appears in Eq. 4.F.1b. The variable  $\vec{r}_{np}$  is the relative coordinate of the proton and the neutron (see Fig. 4.F.1).

The transition matrix element can now be written as

$$\begin{aligned} T_{d,p} &= \langle \psi_{M_{A+1}}^{I_{A+1}}(\xi_{A+1}) \chi_p^{(-)}(k_p, \vec{r}_p), V'_\beta \psi_{M_A}^{I_A}(\xi_A) \chi_d^{(+)}(k_d, \vec{r}_d) \rangle \\ &= \sum_{l, I'_A} (I'_A; l) I_{A+1} (I'_A M'_A l M_{A+1} - M' A | I_{A+1} M_{A+1}) \\ &\quad \times \int d\vec{r}_n d\vec{r}_p \chi_p^{*(-)}(k_p, \vec{r}_p) \phi_{M_{A+1}-M'_A}^* (\vec{r}_n) (\psi_{M_A}^{I_A}(\xi_A), V'_\beta \psi_{M'_A}^{I'_A}(\xi_A)) \\ &\quad \times \phi_d(\vec{r}_{np}) \chi_d^{(+)}(k_d, \vec{r}_d) \delta_{I'_A, I_A} \delta_{M'_A, M_A}. \end{aligned} \quad (4.F.2)$$

In the stripping approximation

$$\begin{aligned} V'_\beta &= V_\beta(\xi, \vec{r}_\beta) - \bar{U}_\beta(r_\beta) \\ &= V_\beta(\xi_A, \vec{r}_{pA}) + V_\beta(\vec{r}_{pn}) - \bar{U}_\beta(r_{pA}). \end{aligned} \quad (4.F.3)$$

Then

$$\begin{aligned} (\psi_{M_A}^{I_A}(\xi_A), V'_\beta \psi_{M_A}^{I_A}(\xi_A)) &= (\psi_{M_A}^{I_A}(\xi_A), V_\beta(\xi_A, \vec{r}_{pA}) \psi_{M_A}^{I_A}(\xi_A)) \\ &\quad + (\psi_{M_A}^{I_A}(\xi_A), V_\beta(\vec{r}_{pn}) \psi_{M_A}^{I_A}(\xi_A)) - \bar{U}_\beta(r_{pA}). \end{aligned} \quad (4.F.4)$$

We assume

$$U_\beta(r_{pA}) = (\psi_{M_A}^{I_A}(\xi_A), V_\beta(\xi_A, \vec{r}_{pA}) \psi_{M_A}^{I_A}(\xi_A)). \quad (4.F.5)$$

Of notice that similar difficulties have been faced in connection with the non-local Fock (exchange) potential. As a rule, the corresponding (HF) mean field equations are rendered local making use of the  $k$ -mass approximation or within the framework of Local Density Functional Theory (DFT), in particular with the help of the Kohn-Sham equations (see e.g. Mahaux, C. et al. (1985), Broglia et al. (2004) and refs. therein; <sup>see also App. 4.A</sup>) Although much of the work in this field is connected with the correlation potential (interweaving of single-particle and collective motion), an important fraction is connected with the exchange potential.

In any case, and returning to the subject of the present appendix, it is always useful to be able to introduce approximations which can help the physics which is at the basis of the phenomenon under discussion (single-particle motion) emerge in a natural way, if not to compare in detail with the experimental data. Within this context, to reduce the integral (4.F.9) one can assume that the proton-neutron interaction  $V_{np}$  has zero-range, i.e.

$$V_{np}(\vec{r}_{np})\phi_d(\vec{r}_{np}) = D_0\delta(\vec{r}_{np}) \quad (4.F.15)$$

so that  $B_m^l$  becomes equal to

$$B_m^l(\theta) = D_0 \int d\vec{r} \chi_p^{*(-)}(k_p, \vec{r}) Y_m^{*l}(\hat{r}) u_l(r) \chi_d^{(+)}(k_d, \vec{r}), \quad (4.F.16)$$

which is a three dimensional integral, but in fact essentially a one-dimensional integral, as the integration over the angles can be worked out analytically.

#### 4.F.1 Plane-wave limit

If in Eq. (4.F.14) one sets  $\bar{U} = 0$ , the distorted waves become plane waves i.e.

$$\chi_d^{(+)}(k_d, \vec{r}) = e^{i\vec{k}_d \cdot \vec{r}}, \quad (4.F.17a)$$

$$\chi_d^{*(-)}(k_p, \vec{r}) = e^{-i\vec{k}_p \cdot \vec{r}}. \quad (4.F.17b)$$

Equation (4.F.16) can now be written as

$$B_m^l = D_0 \int d\vec{r} e^{i(\vec{k}_d - \vec{k}_p) \cdot \vec{r}} Y_m^{*l}(\hat{r}) u_l(r). \quad (4.F.18)$$

The linear momentum transferred to the nucleus is  $\vec{k}_d - \vec{k}_p = \vec{q}$ . Let us expand  $e^{i\vec{q} \cdot \vec{r}}$  in spherical harmonics, i.e.

$$\begin{aligned} e^{i\vec{q} \cdot \vec{r}} &= \sum_l i^l j_l(qr) (2l+1) P_l(\hat{q} \cdot \hat{r}) \\ &= 4\pi \sum_l i^l j_l(qr) \sum_m Y_m^{*l}(\hat{q}) Y_m^l(\hat{r}), \end{aligned} \quad (4.F.19)$$



and

$$r_{Bc} = \sqrt{\left(\frac{b}{A} r_{bc} \sin \theta\right)^2 + \left(\frac{a+B}{B} r_{aA} + \frac{b}{A} r_{bc} \cos \theta\right)^2}. \quad (4.G.65)$$

By the way, (4.G.61) can also be used when particle  $b$  populates a resonant state in the continuum of nucleus  $B$ .

### Appendix 4.H Modified formfactors

- 4.H.1 Two-particle transfer
- 4.H.2 One-particle transfer
- 4.H.3 Inelastic scattering
- 4.H.4 Elastic scattering

*equal to 1*

### Appendix 4.I Dynamical shell model in a nutshell

In the extreme shell model the nucleons move independently, feeling the presences of the other nucleons when bouncing elastically off the nuclear surface of the average potential. The properly normalized probability for removing nucleon from such orbitals is one for  $\omega$  equal to the (unperturbed) energy of the orbital and zero otherwise. (cf. Fig 4.I.1)

In the dynamical shell model (cf. Mahaux, C. et al. (1985) and references therein) the nucleons can bounce inelastically off the nuclear surface setting the nucleus in a vibrational state and changing the state of motion (Fig. 4.I.1). In this case the strength of the levels becomes in general distributed over a range of energies both below and above the Fermi energy. That is, the state  $k$  is found both in the system  $(A - 1)$  produced in a pick-up process and in the system  $(A + 1)$  populated through a stripping reaction as indicated in Fig 4.I.1.

It is still an open question whether this distribution is concentrated in discrete states or displays a continuous behavior. Both situations can in principle be found depending of whether the original single-particle state is close or far away from the Fermi energy. The sum of the spectroscopic factors associated with all the states excited in the pick-up process of a nucleon with quantum numbers  $k$  gives the occupation number associated with the orbital, i.e.  $\int_{-\infty}^{\epsilon_F} S_h(k; \omega) d\omega = n_k$ , where  $S_h$  is the (hole) strength function. The full single-particle strength is found adding to this quantity the spectroscopic factors associated with the excitation of states in the  $(A + 1)$  system where a particle with quantum numbers  $k$  is deposited in the target.

It is noted that the fact that in the dynamical shell model the single-particle strength is distributed not only over an energy range in the  $(A - 1)$  system but also in the  $(A + 1)$  system is intimately connected with the ground state correlations associated with the vibrational modes which produce particle-hole excitations in

*in question*

*their neglect correction  
i.e. leave  $k$*

*\* )*

The trend of the effective masses shown in Fig. 4.I.1 (d) can be quantitatively understood as follows. For single-particle states close to the Fermi energy the intermediate states have all energies larger than the unperturbed single-particle energy, and the resulting shape is  $\delta$ -like with a tail extending away from the Fermi energy. For single-particle orbital 5–7 MeV away from  $\epsilon_F$  there are a number of intermediate states which have the same energy of the initial state leading to zero energy denominators and thus to a marked structure in the strength function. Finally, for single-particle states far away from  $\epsilon_F$ , the density of intermediate states is so large that the matrix elements of these couplings average out to a constant with a value much larger than typical distances between successive intermediate states. These are the conditions which lead to a Breit–Wigner shape.

It is then to be expected that the single-particle levels in the intermediate region will be associated with strength functions which deviate much from a smooth function and for which comparatively large errors can be made through a Breit–Wigner fitting. This is also seen from Fig. 4.I.1 (d) where the effective mass becomes smaller than one, indicating that the area of the fitted shapes are larger than that of the original strength function  $S(k; \omega)$ . This result emphasizes the difficulties found in trying to translate effective masses into spectroscopic factors in a general situation.

Starting from the extreme picture shown in Fig. 4.I.1 (a) where the relation  $\omega = \hbar^2 k^2 / 2m$  holds one arrives at the picture (c) where the relation  $d\omega = \hbar^2 k \delta k / m^*$  again accounts for the main properties of the single-particle motion and where the effect of the couplings are contained in  $m^*$  (see Eq. (4.A.3)). The numerical implementation of the single-particle self-energies scenario have been carried out for different regions of the mass table. In particular, for the valence levels of  $^{208}\text{Pb}$ . In this case the mass operator associated with each orbital was calculated as a function of the energy. The numerical derivative of the real part of the mass operator was then calculated and the  $\omega$ -dependent effective mass obtained as a function of the energy.

The question then arises of how to define an average quantity which depends only on the energy of the orbital and is state independent. Rather different prescriptions have been used to deal with the question. In any case the main result obtained was that the  $\omega$ -dependent effective mass shows a well defined peak at the Fermi surface, its maximum value being considerably larger than one ( $\approx 1.4$ ). The associated full width at half maximum is of the order of 10 MeV. This quantity is much smaller than the Fermi energy ( $\sim 36$  MeV) and is essentially determined by the energy of the low-lying collective modes and of the single-particle gap around  $^{208}\text{Pb}$ .

## Bibliography

- P. W. Anderson. *Basic notions of condensed matter physics*. Benjamin, Menlo Park, California, 1984.

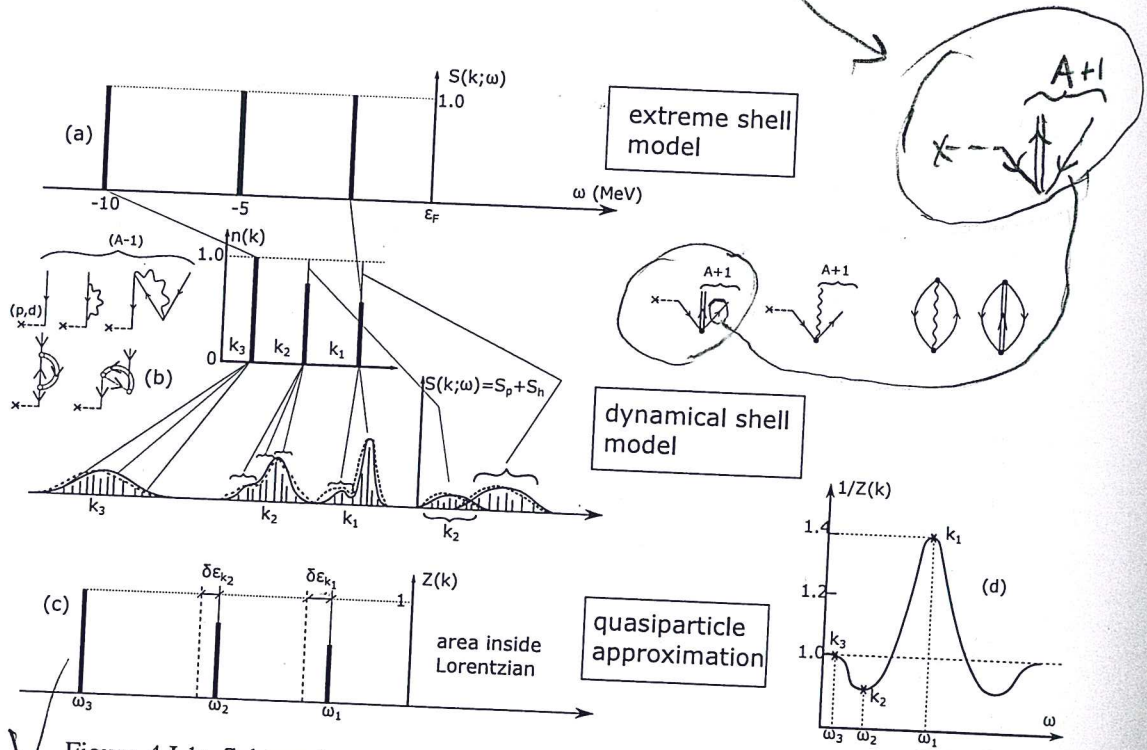
(particle)

single-particle

a pagina 307

*Correct*

### BIBLIOGRAPHY



✓ Figure 4.I.1: Schematic representation of the main quantities characterizing the single-particle motion in the nuclear shell model taking into account the residual interaction among the particles at different levels of approximation. In (a) the interaction is treated in the Hartree-Fock approximation and the particles feel the presence of the other particles through their own confinement in the average field. The strength function shows sharp peaks, each of them carrying the full strength of the states. In fact, the occupation number associated with each state  $k$  contains only one contribution. In (b) the particles still couple only with the average field. However in this case they can set the surface into vibrations by changing its state of motion. The strength associated with each orbital is distributed over a finite energy range. The corresponding occupation numbers arise from the sum of many contributions. Fitting a Lorentzian shape to each peak one can regain the simplicity of the extreme shell model by defining new levels with energy equal to that of the centroid and strength equal to that of the area covered by the Lorentzian shape (cf. (c)). In (d) the energy variation of the shift of the centroids is contained into an effective  $\omega$ -mass according to the standard relation  $\frac{m_\omega}{m} = \left(1 - \frac{\partial \Delta E}{\partial \hbar \omega}\right)$  (see Eq. (4.A.5)). The resulting curve resembles the shape obtained by calculating the inverse of the area below the different Lorentzians (quasiparticle approximation).

use in the paper  
from bare to renorm..

310

## BIBLIOGRAPHY

- ✓ Fernández-García, J.P., M. Rodríguez-Gallardo, M. Alvarez, and A. Moro. Long range effects on the optical model of  $^6\text{He}$  around the Coulomb barrier. *Nuclear Physics A*, 840:19, 2010.
- ✓ H. Feshbach. Unified Theory of Nuclear Reactions. *Annals of Physics*, 5:357, 1958.
- ✓ R. Feynman. *Theory of fundamental processes*. Benjamin, Reading, Mass., 1975.
- ✓ Fröhlich, H. Interaction of electrons with lattice vibrations. *Proc. Royal Soc.*, 215:291, 1952.
- ✓ Glendenning, N. K. *Direct nuclear reactions*. World Scientific, Singapore, 2004.
- ✓ I. Hamamoto. Single-particle components of particle-vibrational states in the nuclei  $^{209}\text{Pb}$ ,  $^{209}\text{Bi}$ ,  $^{207}\text{Pb}$  and  $^{207}\text{Tl}$ . *Nuclear Physics A*, 141:1, 1970.
- ✓ Idini, A. Renormalization effects in nuclei. *Ph.D. thesis, University of Milan*, 2013. *ref net address*
- ✓ Idini, A., F. Barranco, and E. Vigezzi. Quasiparticle renormalization and pairing correlations in spherical superfluid nuclei. *Phys. Rev. C*, 85:014331, 2012.
- ✓ Idini, A., G. Potel, Barranco, E. Vigezzi, and R. A. Broglia. Dual origin of pairing in nuclei. *arXiv:1404.7365v1 [nucl-th]*, 2014.
- ✓ Jennings, B. Non observability of spectroscopic factors. *arXiv: 1102.3721v1 [nucl-th]*, 2011.
- ✓ Jeppesen, H. B. et al. Experimental investigation of the  $^9\text{Li}+\text{d}$  reaction at REX-ISOLDE. *Nucl. Phys. A*, 738:511, 2004.
- ✓ Mahaux, C., P. F. Bortignon, R. A. Broglia, and C. H. Dasso. Dynamics of the shell model. *Physics Reports*, 120:1–274, 1985.
- ✓ A. Migdal. Interaction between electrons and lattice vibrations in a normal metal. *Soviet Physics JETP*, 7:996, 1958.
- ✓ D. Montanari, L. Corradi, S. Szilner, G. Pollaro, E. Fioretto, G. Montagnoli, F. Scarlassara, A. M. Stefanini, S. Courtin, A. Goasduff, F. Haas, D. Jelavić Malenica, C. Michelagnoli, T. Mijatović, N. Soić, C. A. Ur, and M. Varga Pajtler. Neutron Pair Transfer in  $^{60}\text{Ni} + ^{116}\text{Sn}$  Far below the Coulomb Barrier. *Phys. Rev. Lett.*, 113:052501, 2014.
- ✓ B. R. Mottelson. *Elementary Modes of Excitation in Nuclei, Le Prix Nobel en 1975*. Imprimerie Royale Norstedts Tryckeri, Stockholm, 1976. p. 80.
- ✓ Orrigo, S. E. A. and H. Lenske. Pairing resonances and the continuum spectroscopy of  $^{10}\text{Li}$ . *Phys. Lett. B*, 677:214, 2009.

Check  
if published